NASA Contractor Report 181883
ICASE Report No. 89-55

ICASE

ON THE LARGE-EDDY SIMULATION OF TRANSITIONAL WALL-BOUNDED FLOWS

Ugo Piomelli
Thomas A. Zang
Charles G. Speziale
M. Y. Hussaini

Contract No. NAS1-18605
August 1989

Institute for Computer Applications in Science and Engineering
NASA Langley Research Center
Hampton, Virginia 23665-5225

Operated by the Universities Space Research Association

National Aeronautics and
Space Administration

Langley Research Center
Hampton, Virginia 23665-5225

ON THE LARGE-EDDY SIMULATION OF TRANSITIONAL WALL-BOUNDED FLOWS

Ugo Piomelli*
Department of Mechanical Engineering
University of Maryland
College Park, MD 20742

Thomas A. Zang,
NASA Langley Research Center
Hampton, VA 23665

Charles G. Speziale and M. Y. Hussaini*
ICASE, NASA Langley Research Center
Hampton, VA 23665

Abstract

The structure of the subgrid scale fields in plane channel flow has been studied at various stages of the transition process to turbulence. The residual stress and subgrid scale dissipation calculated using velocity fields generated by direct numerical simulations of the Navier-Stokes equations are significantly different from their counterparts in turbulent flows. The subgrid scale dissipation changes sign over extended areas of the channel, indicating energy flow from the small scales to the large scales. This reversed energy cascade becomes less pronounced at the later stages of transition. Standard residual stress models of the Smagorinsky type are excessively dissipative. Rescaling the model constant improves the prediction of the total (integrated) subgrid scale dissipation, but not that of the local one. Despite the somewhat excessive dissipation of the rescaled Smagorinsky model, the results of a large eddy simulation of transition on a flat-plate boundary layer compare quite well with those of a direct simulation, and require only a small fraction of the computational effort. The inclusion of non-dissipative models, which could lead to further improvements, is proposed.

*This research was supported by the National Aeronautics and Space Administration under NASA Contract No. NAS1-18605 while the authors were in residence at the Institute for Computer Applications in Science and Engineering (ICASE), NASA Langley Research Center, Hampton, VA 23665.

1. Introduction

The transition from laminar to turbulent flow has been the subject of much research. Experiments, theoretical studies and numerical methods have been brought to bear on the subject. Direct numerical simulations (DNS) of the Navier-Stokes equations are particularly useful for the study of the late stages of transition, in which nonlinear effects become significant and linear theory as well as perturbation methods fail. This technique has been used to study the structure of the detached shear layer and lambda vortices that arise due to the secondary instability,[1–4] and the effects of heating,[5] streamwise vortices[6] and curvature.[7] Recently, Gilbert and Kleiser[8] have carried out the direct simulation of channel flow at a Reynolds number $Re_c = 5000$ (based on centerline velocity and channel halfwidth) for the full transition process from laminar to turbulent flow.

Direct simulation of the governing equations has so far been limited to simple flows and low Reynolds numbers due to the massive computational effort it requires; the use of two million grid points is not uncommon, and simulations have been performed with up to five million points.[9] In general, more resolution is required to study the later stages of transition than for a turbulent flow, since in the former case it is essential to distinguish between truly chaotic behavior and grid-scale fluctuations caused by insufficient resolution. This resolution requirement makes the application of direct simulation to the study of flows of engineering interest unfeasible, at least in the near future; less computationally intensive methods are required for engineering applications.

A technique that has been successfully applied to the study of turbulent flows is large-eddy simulation (LES). In LES one accurately resolves only the large, energy-carrying scales of the motion and models the effect of the small scales (subgrid scales), which appears in a residual stress term. In turbulent flows, the small scales tend to be more isotropic and homogeneous than the large scales, and do not depend very strongly on the boundary conditions. For these reasons their effect can be represented by simpler models than the currently used turbulence models. Large-eddy simulations have been successfully applied to a variety of turbulent, wall-bounded flows such as plane channel flow,[10–12] boundary layers[13] and channel flow with transpiration.[14] The only applications of this technique to transitional flows to date are due to Horiuti,[15] Dang and Deschamps[16] and Deschamps and Dang.[17]

Horiuti[15] used a simple residual stress model to extend his direct simulations to the later stages of transition. The model that he employed, the Smagorinsky[18] model, dissipates a significant amount of turbulent energy from the resolved scales, effectively slowing down the transition process. Horiuti's results are, therefore, only qualitatively correct, due to the significant inaccuracies of the residual stress model.

In two related papers Dang and Deschamps[16] and Deschamps and Dang[17] describe their large-eddy simulation of transitional flow. Their results are inconclusive: they do not make any comparison with theoretical predictions at the early stages of transition, and, at the later

stages, compare their LES results with those of a direct simulation that they also performed. Their DNS results, however, compare quite poorly with experimental data, perhaps due to insufficient resolution, and no conclusive statement can be made regarding the accuracy of their large-eddy simulation.

It is the purpose of the present paper to establish a rational basis for the application of LES to transitional flows. This will be done by examining the results of direct simulations of transitional channel flow to understand the physical behavior of the subgrid scale structures. The energy exchange between subgrid scales and large scales will be studied and compared with turbulent flow behavior. It will be shown that the interaction between large and small scales in transitional flows is quite different than in turbulent flows.

In Section 2 the governing equations will be laid out and basic considerations for the optimal choice of filter for the LES of transitional flows will be made. In Section 3, the direct simulation databases will be examined in detail, and residual stresses and subgrid scale dissipation will be calculated and presented. Commonly used residual stress models will be evaluated in Section 4, and preliminary results of a large-eddy simulation of a transitional flat-plate boundary layer flow will be discussed in Section 5. Conclusions and recommendations for future work will be made in the last section.

2. Numerical formulation

In large-eddy simulations we decompose the flow variables (velocity u_i and pressure p) into a large scale component (denoted by an overbar) and a subgrid scale component. The large scale field is defined by the filtering operation:

$$\overline{f}(x_1, x_2, x_3) = \int_D \prod_{i=1}^{3} G_i(x_i, x_i') f(x_1', x_2', x_3') dx_1' dx_2' dx_3' \tag{1}$$

where the integral is extended over the entire domain D and G_i is the filter function in the ith direction.[19]

The filtered Navier-Stokes and continuity equations, which describe the evolution of the large, energy-carrying eddies, can be obtained by applying the filtering operation to the incompressible Navier-Stokes and continuity equations to yield

$$\frac{\partial \overline{u}_i}{\partial t} + \frac{\partial}{\partial x_j}\left(\overline{\overline{u}_i \overline{u}_j}\right) = -\frac{\partial \overline{p}}{\partial x_i} - \frac{\partial \tau_{ij}}{\partial x_j} + \frac{1}{Re}\frac{\partial^2 \overline{u}_i}{\partial x_j \partial x_j} \tag{2}$$

$$\frac{\partial \overline{u}_i}{\partial x_i} = 0, \tag{3}$$

in which a reference length and velocity scale are used to make $\overline{u}_i$, $\overline{p}$, x_i and t dimensionless.

The effect of the subgrid scales appears in the residual (or subgrid scale) stress

$$\tau_{ij} = \overline{u_i u_j} - \overline{\overline{u}_i \overline{u}_j}. \tag{4}$$

The residual stress can be further decomposed into the cross stress C_{ij} and the subgrid scale Reynolds stress R_{ij}, given by

$$C_{ij} = \overline{\overline{u}_i u'_j} + \overline{\overline{u}_j u'_i} \tag{5}$$

$$R_{ij} = \overline{u'_i u'_j} \tag{6}$$

respectively, in which $u'_i = u_i - \overline{u}_i$ is the subgrid scale velocity. In addition, the Leonard stress L_{ij} is defined as

$$L_{ij} = \overline{\overline{u}_i \overline{u}_j} - \overline{u}_i \overline{u}_j. \tag{7}$$

The cross stress C_{ij} and subgrid scale Reynolds stress R_{ij} are invariably modeled, while the Leonard stress L_{ij} can be either computed or modeled.

Most of the models currently in use correlate the residual stress with the large scale strain-rate tensor $\overline{S}_{ij}$,

$$\overline{S}_{ij} = \frac{1}{2}\left(\frac{\partial \overline{u}_i}{\partial x_j} + \frac{\partial \overline{u}_j}{\partial x_i}\right) \tag{8}$$

which, in incompressible flow, is traceless. The trace of the residual stress tensor is, therefore, commonly incorporated into the total pressure, and only the anisotropic part of the residual stress tensor

$$\tau^a_{ij} = \tau_{ij} - \delta_{ij}\tau_{kk}/3, \tag{9}$$

(in which $\tau_{kk} \equiv q^2_{sgs}$ is the subgrid scale kinetic energy and δ_{ij} is Kronecker delta) requires modeling.

For the large-eddy simulation of turbulent flows, the most commonly used filters are the Gaussian filter, the sharp Fourier cutoff filter and the box filter. The Gaussian filter is defined as

$$G_i(x_i, x'_i) = \left(\frac{6}{\pi \Delta_i^2}\right)^{1/2} \exp\left[\frac{-6(x_i - x'_i)^2}{\Delta_i^2}\right], \tag{10}$$

where Δ_i is the filter width in the ith direction, usually related to the grid size Δx_i.

The sharp Fourier cutoff filter is most conveniently defined in Fourier space:

$$\widehat{G}_i(k_i) = \begin{cases} 1 & \text{for } k_i < K_{ci} \\ 0 & \text{otherwise} \end{cases} \tag{11}$$

in which $\widehat{G}_i(k_i)$ is the Fourier coefficient of the filter function G_i, and K_{ci} is the cutoff wavenumber in the ith direction, that is related to the filter width by $K_{ci} = \pi/\Delta_i$.

The variable-width box filter is defined as

$$G_i(x_i, x_i') = \begin{cases} 1/\Delta_i & \text{for } |x_i - x_i'| \leq \Delta_i/2 \\ 0 & \text{otherwise.} \end{cases} \tag{12}$$

All of the filters defined above have been used for the large-eddy simulation of turbulent wall-bounded flows.

When either the Gaussian or the box filter is used, the subgrid scales must represent both large and small scales of motion.[12] When the cutoff filter is used, on the other hand, the subgrid scales only contain the effect of the structures with wavenumber larger than the cutoff wavenumber K_{ci}. This characteristic of the cutoff filter is very desirable for the large-eddy simulation of transitional flows, in which the large scales of motion (such as the Tollmien-Schlichting waves) must be resolved very accurately, and large eddy simulation should give the same results as direct simulation in the early stages of transition.

It is also useful to remark that the sum of the cross stress, Leonard stress and subgrid scale Reynolds stress is invariant to a Galilean transformation, regardless of the filter used.[20] The subgrid scale Reynolds stress R_{ij} has the same property. The Galilean invariance properties of Leonard and cross stresses, however, depend on the type of filter used. If either the Gaussian or the variable-width box filter is employed, neither the Leonard stresses nor the cross stresses are Galilean invariant, but their sum is. On the other hand, if the cutoff filter is used, both Leonard and cross stresses are Galilean invariant.

3. Analysis of databases

To gain a better understanding of the structure of the residual stress tensor in transitional flows, one can use the results of direct simulations to evaluate the residual stresses, and study their behavior at various stages of transition, by comparing the exact residual stress, obtained from (9) and (4), with the predictions of a model. This technique, which is known as an *a priori* test, was first applied by Clark, Ferziger and Reynolds[21] to the study of homogeneous, isotropic turbulence. To calculate the exact residual stress, the velocity field obtained from a direct simulation of the Navier-Stokes equations is filtered using one of the filters defined above to yield the large scale velocity field $\overline{u}_i$; the subgrid scale velocity field u_i' can next be obtained by subtracting $\overline{u}_i$ from u_i. The large scale and subgrid scale velocities can then be used to calculate the exact values of quantities of interest such as the residual stress τ_{ij} [which can be obtained from (4)] and the dissipation by the residual stresses

$$\epsilon_{sgs} = \tau_{ij}\overline{S}_{ij} = \tau_{ij}^a\overline{S}_{ij}. \tag{13}$$

This term, which appears as a dissipation term in the transport equation for the resolved energy and as a production term in the transport equation for the subgrid scale energy,

represents the energy transferred from large scales to subgrid scales (the "energy cascade" in turbulent flow). It has been argued[22] that, as long as a subgrid scale model drains energy from the large scales at the correct rate, its overall performance will be acceptable even if the model fails to predict the local stress accurately; the considerable success obtained by large-eddy simulations which use the Smagorinsky[18] model has been attributed to this characteristic. Finally, the filtered field $\overline{u}_i$ can be used to compute the predictions of the various models, which can then be compared with the exact quantities.

Although the *a priori* test gives useful indications regarding the behavior of subgrid-scale quantities, its results should not be considered final. The ultimate test of the accuracy of a residual stress model is *a posteriori*, when the model is used in a large-eddy simulation and its results are compared with experimental and numerical results.

In the present work we have used numerical databases similar to those generated by Zang and Krist[9] to study the behavior of the components of the residual stress tensor and of the subgrid scale dissipation during transition in incompressible plane channel flow (a schematic representation of the channel geometry is shown in Figure 1). The velocity field from the direct simulation, which had been obtained at $Re_c = 8000$ was filtered using the cutoff filter in the xz-plane; no filtering was applied in the normal direction. The simulation was started with a parabolic velocity profile, on which a 2D and 3D disturbance were superimposed. The 2D disturbance was a Tollmien-Schlichting wave with a wavenumber $\alpha_x = 1$ (made dimensionless by the channel halfwidth δ) and an amplitude of 2%. The wavenumbers of the 3D disturbance were respectively $\alpha_x = 1$ and $\alpha_z = 1.5$; its amplitude was 0.02%, and its phase was matched with that of the 2D wave. The mass flux through the channel was maintained constant and equal to its laminar value. Channel flow databases where preferred to boundary layer databases for the *a priori* test because channel flow can be computed far more economically than boundary layer transition.

As a preliminary step, the effect of the filter width on the *a priori* test results was studied. It was found that changing the filter width has two principal effects: in the first place, the amount of energy contained in the subgrid scales changes, as does their percentage contribution to the residual stress tensor. Moreover, removal of particular waves may result in slightly different residual stress profiles. The qualitative behavior of subgrid scale statistics, however, is not much influenced by the filter width; for this reason in the remainder of this study we will only present results obtained with a single filter width, corresponding to cutoff wavenumbers $K_{c1} = K_{c3} = 9$.

Five flow realizations were examined at times $t = 175$, 180, 185, 190 and 196 (made dimensionless by the centerline velocity U_c and channel halfwidth). This covers the period from the development of the so-called "second spike" (at $t = 175$), through the start of the laminar breakdown (at $t = 185$), into the transitional region ($t = 196$). The transition process itself is not complete until $t = 240$. The Reynolds stress $< u''v'' >$ (where $u_i'' = u_i - U_i$

is the turbulent fluctuation in the ith direction, $U_i = < u_i >$, and $< . >$ represents an average over the xz-plane) reaches a maximum at $t = 210$. By $t = 196$, $< u''v'' >$ is approximately two thirds of its maximum value, and is nearly twice the final turbulent value. In all cases the velocity, which had been computed on grids using up to 216×192×216 grid points, was filtered onto an 18×192×18 grid.

In Figure 2, the temporal histories of the subgrid scale kinetic energy q^2_{sgs} are shown, along with its ratio to the total turbulent kinetic energy $q^2 = u''_i u''_i$. At the late stages of transition the subgrid scale energy increases rapidly, as small scale structures are generated. For $t > 180$, subgrid scales account for almost 30% of the total energy. This result indicates that a finer mesh than the one used for the *a priori* test is required to resolve the late stages of transition.

The (1,2)-component of the residual stress tensor is shown in Figure 3; the residual stress is less than 20% of the total stress (except in the near-wall region). For $t \leq 180$, the residual stress changes sign at approximately $y/\delta = -0.8$; this behavior is not observed in turbulent flows. At later times the sign change present at the early stages disappears and, as small scale structures are generated in the near-wall region, the residual stress increases there.

The sign reversal in the residual stress suggests that the energy cascade may be reversed, at least locally, in transitional flows: energy may flow from small scales to large scales. This hypothesis is supported by an examination of the subgrid scale dissipation (Figure 4). Although the mean dissipation is always negative (indicating that, on the average, the small scales absorb energy from the large ones) the fact that, for $t \leq 180$, the root-mean-square dissipation is approximately five times as large as the mean indicates that the reversed energy flow is significant in considerable regions of the channel. To clarify this point further, the the area of each xz-plane over which ϵ_{sgs} is positive, A_+ was calculated, and its ratio to the total area of an xz-plane, A_t, is shown in Figure 5 at $t = 175$. In almost half of the channel, at this time, energy is flowing from the small scales to the large ones. At its peak, the rms dissipation by the subgrid scales is approximately 65% of the mean viscous dissipation $\epsilon_v = -2\overline{S}_{ij}\overline{S}_{ij}/Re$, and 60% of the rms viscous dissipation. As transition progresses, however, the subgrid scales become more dissipative, especially in the near-wall region. At $t = 196$ the rms ϵ_{sgs} is only 80% larger than the mean, indicating that the regions of reversed energy flow are much reduced in extent and intensity.

4. Modeling considerations

The most commonly used residual stress models for large-eddy simulations of turbulent flows are modifications of the Smagorinsky[18] model for the anisotropic part of the residual

stress. The Smagorinsky model is an eddy viscosity model which relates the modeled residual stress τ_{ij}^m to the strain-rate tensor $\overline{S}_{ij}$ through an eddy viscosity ν_T:

$$\tau_{ij}^m = -2\nu_T \overline{S}_{ij} \tag{14}$$

in which ν_T is given by

$$\nu_T = \ell^2 \sqrt{2\overline{S}_{ij}\overline{S}_{ij}} \tag{15}$$

and ℓ is a subgrid length scale, that is usually related to the filter width by

$$\ell = C_S \left(\Delta x \Delta y \Delta z\right)^{1/3}, \tag{16}$$

where the Smagorinsky constant C_S is set equal to 0.1 for wall bounded flows.

The Smagorinsky model is absolutely dissipative. Computed subgrid scale dissipations are shown in Figure 6, and their integrated values over the entire computational domain are given in Table I. The model is incapable of predicting the reverse cascade regions, and overestimates the subgrid scale dissipation. Part of the problem is due to the fact that the model is only based on large scale quantities, and predicts nonzero residual stresses even in laminar flow. This limitation can be overcome in many ways. One can, for example, scale the modeled stress according to the stage of transition the flow is undergoing; the constant C_S, for example, can be multiplied by the factor $(H_l - H)/(H_l - H_t)$, where $H = \delta^*/\theta$ is the shape factor, δ^* is the displacement thickness, θ the momentum thickness, and the subscripts l and t refer respectively to laminar and fully developed turbulent flow. For laminar flow, $H_l = 5/2$, while, for $Re_c = 8000$, $H_t \simeq 1.7$.[23] The length scale ℓ can then be given by

$$\ell = C_S \frac{H_l - H}{H_l - H_t} \left(\Delta x \Delta y \Delta z\right)^{1/3}. \tag{17}$$

In turbulent flows the length scale is often multiplied by a van Driest damping function[24] to account for the fact that the growth of even the large structures is inhibited by the presence of the wall. The length scale ℓ then becomes

$$\ell = C_S \left[1 - \exp(-y^+/25)\right] \left(\Delta x \Delta y \Delta z\right)^{1/3} \tag{18}$$

where y^+ is the distance from the wall made dimensionless by the shear velocity $u_\tau = (\tau_w/\rho)^{1/2}$ (where τ_w is the wall stress) and kinematic viscosity ν. Although this approach yields non-zero residual stresses even in laminar flow, these stresses are very small due to the small value of the shear velocity (and, therefore, of y^+) in laminar flow. In laminar flow, the subgrid scale dissipation is 35% of the viscous dissipation if (16) is used, zero if (17) is used and 7% of the viscous dissipation if (18) is used.

Although the introduction of damping improves somewhat the prediction of the integrated dissipation (see Table I), the reversed energy flow is still not permitted, and the

dissipation is not well predicted locally. At later stages, all models underpredict the subgrid scale effects. The use of damping would probably lead to a more realistic prediction of the early transition process than the straightforward Smagorinsky model used, for example, by Horiuti.[15] However, the time development of single structures would probably still be incorrectly predicted, since their growth rate would be damped where the model is excessively dissipative, and amplified where the model is not dissipative enough.

Two models that have the capability of generating positive dissipation (*i.e.*, reversed energy flow) are the mixed model[25] and the nonlinear eddy viscosity model.[26] The mixed model is commonly written as

$$\tau_{ij}^m = C_B \left(\overline{u}_i \overline{u}_j - \overline{\overline{u}}_i \overline{\overline{u}}_j \right) - 2\nu_T \overline{S}_{ij} \tag{19}$$

and has been successfully applied to the large-eddy simulation of turbulent flows.[12,25] The model in this form cannot be used with the cutoff filter, which has the property that $\overline{u}_i = \overline{\overline{u}}_i$. A modification of this model, which can be used with the cutoff filter, is

$$\tau_{ij}^m = C_B \left(\overline{u}_i - \widetilde{u}_i \right) \left(\overline{u}_j - \widetilde{u}_j \right) - 2\nu_T \overline{S}_{ij} \tag{20}$$

in which $\widetilde{u}_i$ represents the velocity filtered using a sharp cutoff filter with a cutoff wavenumber $K'_{ci} < K_{ci}$; here the Galilean invariance constraint is satisfied for any value of C_B.

The nonlinear eddy viscosity model[26] takes the form

$$\tau_{ij}^m = -2q\ell\overline{S}_{ij} - C_D\ell^2 \left(\overline{S}_{ik}\overline{S}_{kj} - \frac{1}{3}\overline{S}_{mn}\overline{S}_{mn}\delta_{ij} \right) - C_E\ell^2 \left(\overset{\circ}{\overline{S}}_{ij} - \frac{1}{3}\overset{\circ}{\overline{S}}_{mm}\delta_{ij} \right) \tag{21}$$

where q is a velocity scale and $\overset{\circ}{\overline{S}}_{ij}$ is the Oldroyd derivative of $\overline{S}_{ij}$:

$$\overset{\circ}{\overline{S}}_{ij} = \frac{\partial \overline{S}_{ij}}{\partial t} + \overline{u}_k \frac{\partial \overline{S}_{ij}}{\partial x_k} - \frac{\partial \overline{u}_i}{\partial x_k}\overline{S}_{kj} - \frac{\partial \overline{u}_j}{\partial x_k}\overline{S}_{ki}. \tag{22}$$

This nonlinear model has never been applied to large-eddy simulations of turbulent flow, although it gave more accurate predictions than the commonly used models when employed as a standard turbulence model for wall-bounded flows.[26]

Both the mixed model and the nonlinear model are not strictly dissipative, so that their use could lead to improved results. They, however, require added empirical information in the form of additional constants and the new cutoff wavenumber K'_{ci}, which must be optimized for turbulent and transitional flows.

The *a priori* tests do not allow us to estimate to what extent the excessive dissipation affects growth rates and the final results, or whether the inclusion of energy-producing terms in the residual stress model is necessary. For this reason, large-eddy simulations which employ various variants of the Smagorinsky model have been carried out to evaluate *a posteriori* the accuracy of the model. These simulations will be discussed in the next section.

5. Large-eddy simulation results

To evaluate more conclusively the effect of dissipation by the subgrid scales on the transition process, two large-eddy simulations have been carried out in which the Smagorinsky[18] model has been used to parameterize the residual stresses. In these simulations the transition process on a flat-plate boundary layer was calculated. The flat-plate boundary layer was preferred over plane channel flow because of the greater similarity this flow has to problems of technological importance in aerodynamics.

The simulations were performed using a spectral collocation method. Fourier expansions were used in the streamwise and spanwise directions, Chebyshev polynomials in the wall-normal direction. The code uses the improved splitting method described in Zang and Hussaini.[27] The time advancement is performed using an implicit Crank-Nicolson method for the diffusion term, residual stresses and incompressibility constraint; a third order Runge-Kutta method is applied to the remaining terms.

The number of grid points used in this simulation was $24\times48\times24$. Initial conditions for the simulation consisted of a Blasius velocity profile, on which a 2D and 3D disturbance were superimposed. The 2D disturbance was a Tollmien-Schlichting wave with a wavenumber $\alpha_x = 0.25$ (made dimensionless by the displacement thickness δ^*) and an amplitude of 1.8%. The wavenumbers of the 3D disturbance were respectively $\alpha_x = 0.25$ and $\alpha_z = 0.209$; its amplitude was 0.8%, and its phase was 36° ahead of the 2D wave. The thickness of the boundary layer was assumed to be constant in the streamwise direction. The filtered Navier-Stokes equations (2)–(3) were integrated for a total time $t/t_{TS} = 4.5$ (made dimensionless by the period of the Tollmien-Schlichting waves t_{TS}). Large-eddy simulation results were compared with those of a direct simulation which used up to $144\times144\times324$ grid points.[28] The direct and large eddy simulation codes were essentially the same; the CPU time required per iteration and grid point was, therefore, the same. Due to the coarser grid used by the LES, however, less than 4 CPU hours were required to advance the solution for 4.5 Tollmien-Schlichting periods. The direct simulation, by comparison, required over 100 CPU hours to integrate the equations for the same period.

The first simulation used the Smagorinsky model (14) with the length scale (18), based on van Driest damping. The dissipation by the subgrid scales was found, in this case, to be excessive. The growth rate ω obtained from the large-eddy simulation is compared in Figure 7 with that of the direct simulation. The growth of the perturbation is significantly damped in the LES, indicating that the effect of the residual stress model is too large.

A new length scale combining Eqs. (17) and (18), was then used:

$$\ell = C_S \frac{H_l - H}{H_l - H_t} (\Delta x \Delta y \Delta z)^{1/3} \left[1 - \exp(-y^+/25)\right] \tag{23}$$

in which $H_l = 2.6$ for the Blasius profile, and H_t was set to 1.4 on the basis of experimental evidence.[29] When this length scale is used, the model is essentially turned off during the early stages of transition; this allows for much more accurate prediction of the early stages of transition. The growth rate predicted by an LES using (23) is compared in Figure 7 with the DNS results. The agreement between the DNS and the LES is good at the early stages. For $2 \leq t/t_{TS} \leq 3.5$ the model appears to dissipate excessively, slowing down the evolution of the perturbation. At later times, as the subgrid scales become more dissipative, the LES predicts an increased growth rate similar to that observed in the DNS results. This increase, however, occurs at a later time, perhaps due to the errors at the intermediate stages of the transition process.

The development of the shape factor H (see Figure 8) follows similar trends: if no scaling is used, H remains at its laminar value throughout the simulation. When scaling is applied in the early stages, the LES results compare well with the DNS ones. The decrease in H that takes place when the mean velocity profile becomes significantly altered by the perturbation velocity occurs at a later time in the LES than observed in the DNS results, possibly because of the poor prediction of the intermediate transition processes.

The harmonic energy content of selected scales is shown in Figure 9. The time evolution of the larger scales of motion (the 2D Tollmien-Schlichting waves are the (1,0) mode, for example) is predicted with surprising accuracy, although, once again, the transition process is delayed by the excessive dissipation. The large scale Reynolds stresses $< \overline{u}_i'' \overline{u}_j'' >$ (where $\overline{u}_i'' = \overline{u}_i - U_i$ is the fluctuating large scale velocity) are also predicted with acceptable accuracy (see Figure 10). It should be noticed that, at this stage and with the mesh used in the present simulation, the subgrid scales account for about 20% of the total turbulent kinetic energy. If one were to compare the LES results with experimental data or with unfiltered DNS results, one should expect that discrepancy. In the present case, the DNS data was filtered onto a $24 \times 48 \times 24$ grid to yield a more significant comparison.

Equal $\partial \overline{u}/\partial y$ contours are shown in Figure 11. Although the large-eddy simulation captures all the essential features of the flow, the liftup of the detached shear layer is not as pronounced, consistent with the delay of the transition process due to the excessively dissipative nature of the residual stress model.

6. Conclusions

A detailed study of the structure of the subgrid scales in transitional plane channel flow has been conducted at various stages of the transition process. It has been demonstrated that the residual stress and subgrid scale dissipation obtained from direct numerical simulation of the Navier-Stokes equations are significantly different from their counterparts in turbulent flows. During transition the subgrid scale dissipation changes sign for considerable areas

of the flow, indicating a reversal of the energy cascade wherein large scales absorb energy from the small ones. It was found that the standard residual stress models are excessively dissipative; they erroneously delay the onset of transition in the large-eddy simulation of boundary layers, leading to considerable error. The use of a shape factor function combined with van Driest damping to form a modified Smagorinsky model for transitional flows was shown to partially alleviate this problem. This new residual stress model was demonstrated to yield results for the disturbance growth rate and energy content of selected harmonics in transitional boundary layers that compared favorably with the direct simulations. These LES results were obtained at a small fraction of the computational expense required for the direct simulation.

The simulations described above were carried out with the intent of determining the feasibility of large-eddy simulations for transitional flows. The fact that the LES results compared reasonably well with DNS results, indicates that this technique can be successfully applied to the simulation of transitional as well as turbulent flows. Since these results were obtained using very simple residual stress models, it appears that in transitional flows (as well as in turbulent flows) accurate calculation of the large scales is of primary importance for the prediction of quantities of engineering interest.

While the results of this study have established the feasibility of large-eddy simulations with relatively simple residual stress models, there is still a need to develop improved models. For example, it may be useful to introduce an intermittency factor based on some large scale kinematic quantity that senses the development of small scale turbulence activity. In this manner, the residual stress model can be turned on or off depending on the local development of turbulence – a feature that could considerably improve the accuracy of transitional LES. The inclusion of non-dissipative models may also be of assistance. Two such models have been proposed: one based on a nonlinear eddy viscosity model and another based on the commonly used mixed model. The calibration and testing of such new models is a substantial research effort that is beyond the scope of the present paper. These, as well as other technical issues, are part of an ongoing research effort on the large-eddy simulation of transitional flows.

REFERENCES

[1]S.A. Orszag, and A.T. Patera, *J. Fluid Mech.* **128**, 347 (1983).

[2]A.A. Wray and M.Y. Hussaini, *Proc. Roy. Soc. London,* series A, **392**, No. 1308, 373 (1984).

[3]L. Kleiser and U. Schumann, *Proc. ICASE Symp. on Spectral Methods*, (R.G. Voigt, D. Gottlieb and M.Y. Hussaini, eds.), SIAM-CBMS:Philadelphia, 141 (1984).

[4]P.R. Spalart and K.S. Yang, *J. Fluid Mech.* **178**, 345 (1987).

[5]T.A. Zang and M.Y. Hussaini, *AIAA Paper No. 85-1698*, 1985.

[6]B.A. Singer, J.H. Ferziger and H.L. Reed, *AIAA Paper No. 87-0048*, (1987)

[7]W.H. Finlay, J.B. Keller and J.H. Ferziger, *AIAA Paper No. 87-0363*, (1987).

[8]N. Gilbert, and L. Kleiser, *Proc. Int. Seminar on Near-Wall Turbulence*, Dubrovnik, Yugoslavia, (1988).

[9]T.A. Zang and S.E. Krist, *Theoretical Comput. Fluid Mech.*, **1**, 41 (1989).

[10]J.W. Deardorff, *J. Fluid Mech.* **41**, 453 (1970).

[11]P. Moin and J. Kim, *J. Fluid Mech.* **118**, 341 (1982).

[12]U. Piomelli, P. Moin and J.H. Ferziger, *Phys. Fluids* **31**(7), 1884 (1988).

[13]L. Schmitt, K. Richter and R. Friedrich, *Finite Approx. in Fluid Mechanics* (E.H. Hirschel, ed.). Vieweg:Braunschweig, 232 (1985).

[14]U. Piomelli, P. Moin and J.H. Ferziger, *AIAA Paper No. 89-0375*, (1989).

[15]K. Horiuti, *J. Phys. Soc. Japan* **55**, No. 5, 1528 (1986).

[16]K. Dang and V. Deschamps, *Proc. 5th Int. Conf. on Numerical Methods in Laminar and Turbulent Flow.* Montréal, Canada, (1987).

[17]V. Deschamps and K. Dang, *Proc. 6th Symp. on Turbulent Shear Flows*, Toulouse, France, (1987).

[18]J. Smagorinsky, *Monthly Weather Review*, **91**, 99 (1963).

[19]In the present work x_1 or x is the streamwise direction, x_2 or y is the wall-normal direction, and x_3 or z is the spanwise direction; u, v and w (or u_1, u_2 and u_3) are the velocity components in the coordinate directions.

[20]C.G. Speziale, *J. Fluid Mech.* **156**, 55 (1985).

[21]R.A. Clark, J.H. Ferziger and W.C. Reynolds, *J. Fluid Mech.* **91**, 1 (1979).

[22] R.S. Rogallo and P. Moin, *Ann. Rev. Fluid Mech.* **16**, 99 (1984).

[23]R.B. Dean, *Jour. Fluids Engng.*, **100**, 215 (1978).

[24]E.R. Van Driest, *J. Aero. Sci.* **23**, 1007 (1956).

[25]J. Bardina, J.H. Ferziger and W.C. Reynolds, *AIAA Paper No. 80-1357*, (1980).

[26]C.G. Speziale, *J. Fluid Mech.* **178**, 459 (1987).

[27]T.A. Zang and M.Y. Hussaini, *Appl. Math. Comp.*, **19**, 359 (1986).

[28]T.A. Zang and M.Y. Hussaini, *Nonlinear wave interactions in fluids* (R.W. Miksad, T.R. Akylas and T. Herbert, eds.), AMD **27**, ASME:New York, 131 (1987).

[29]H. Schlichting, *Boundary layer theory*, MacGraw-Hill:New York (1978).

LIST OF FIGURES

Figure 1. Plane channel flow geometry.

Figure 2. Subgrid scale energy and energy ratio obtained from direct simulations; $\circ$ $t = 175$; $+$ $t = 185$; $\diamond$ $t = 196$; (a) q^2_{sgs}; (b) q^2_{sgs}/q^2.

Figure 3. Residual stress τ_{12} obtained from direct simulations; $\circ$ $t = 175$; $+$ $t = 185$; $\diamond$ $t = 196$; (a) Mean; (b) root-mean-square.

Figure 4. Subgrid scale scale dissipation ϵ_{sgs} obtained from direct simulations; $\circ$ $t = 175$; $+$ $t = 185$; $\diamond$ $t = 196$; (a) Mean; (b) root-mean-square.

Figure 5. Ratio of the area of an xz-plane over which $\epsilon_{sgs} > 0$ to the total area of an xz-plane.

Figure 6. Subgrid scale dissipation ϵ_{sgs}; $\circ$ DNS; $\triangle$ modeled, length scale given by (16); $+$ modeled, length scale given by (17); $\times$ modeled, length scale given by (18). (a) $t = 175$; (b) $t = 185$; (c) $t = 196$.

Figure 7. Time evolution of the disturbance growth rate ω. —— LES, length scale given by (18); ---- LES, length scale given by (23); $\blacksquare$ DNS.

Figure 8. Time evolution of the shape factor H. —— LES, length scale given by (18); ---- LES, length scale given by (23); $\blacksquare$ DNS.

Figure 9. Time evolution of the energy content of selected harmonics. The length scale for the LES was given by (23). (1,0) mode: —— LES, $\circ$ DNS; (1,1) mode: —·— LES, $\triangle$ DNS; (2,0) mode: ····· LES, $+$ DNS; (2,1) mode: ---- LES, $\times$ DNS; (2,2) mode: —·— LES, $\diamond$ DNS.

Figure 10. Large scale Reynolds stresses $\overline{u}_i''\overline{u}_j''$. The length scale for the LES was given by (23). The LES results are at $t/t_{TS} = 4$; the DNS results are at $t/t_{TS} = 3.88$ and are filtered on a 24×48×24 grid. $< \overline{u}''^2 >$: —— LES, $\circ$ DNS; $< \overline{v}''^2 >$: —·— LES, $+$ DNS; $< \overline{w}''^2 >$: ---- LES, $\triangle$ DNS; $< \overline{u}''\overline{v}'' >$: ····· LES, $\times$ DNS.

Figure 11. Contours of $\partial\overline{u}/\partial y$ in the peak xy-plane. (a) DNS at $t/t_{TS} = 3.88$, filtered on a 24×48×24 grid; (b) LES at $t/t_{TS} = 4$, length scale given by (23).

t	ϵ_{sgs} exact	ϵ_{sgs} predicted (ℓ given by (16))	ϵ_{sgs} predicted (ℓ given by (17))	ϵ_{sgs} predicted (ℓ given by (18))
175.	-4.62×10^{-5}	-3.83×10^{-4}	-2.95×10^{-6}	-1.75×10^{-4}
180.	-1.59×10^{-4}	-6.03×10^{-4}	-1.46×10^{-5}	-2.94×10^{-4}
185.	-5.80×10^{-4}	-7.17×10^{-4}	-4.80×10^{-5}	-3.43×10^{-4}
190.	-1.30×10^{-3}	-8.86×10^{-4}	-1.78×10^{-4}	-3.58×10^{-4}
196.	-1.53×10^{-3}	-2.03×10^{-3}	-9.80×10^{-4}	-4.37×10^{-4}

Table I: Dissipation by the subgrid scales.

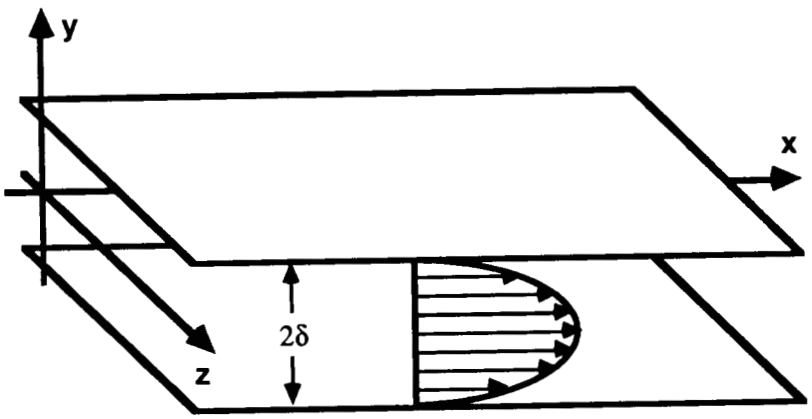

Figure 1. Plane channel flow geometry.

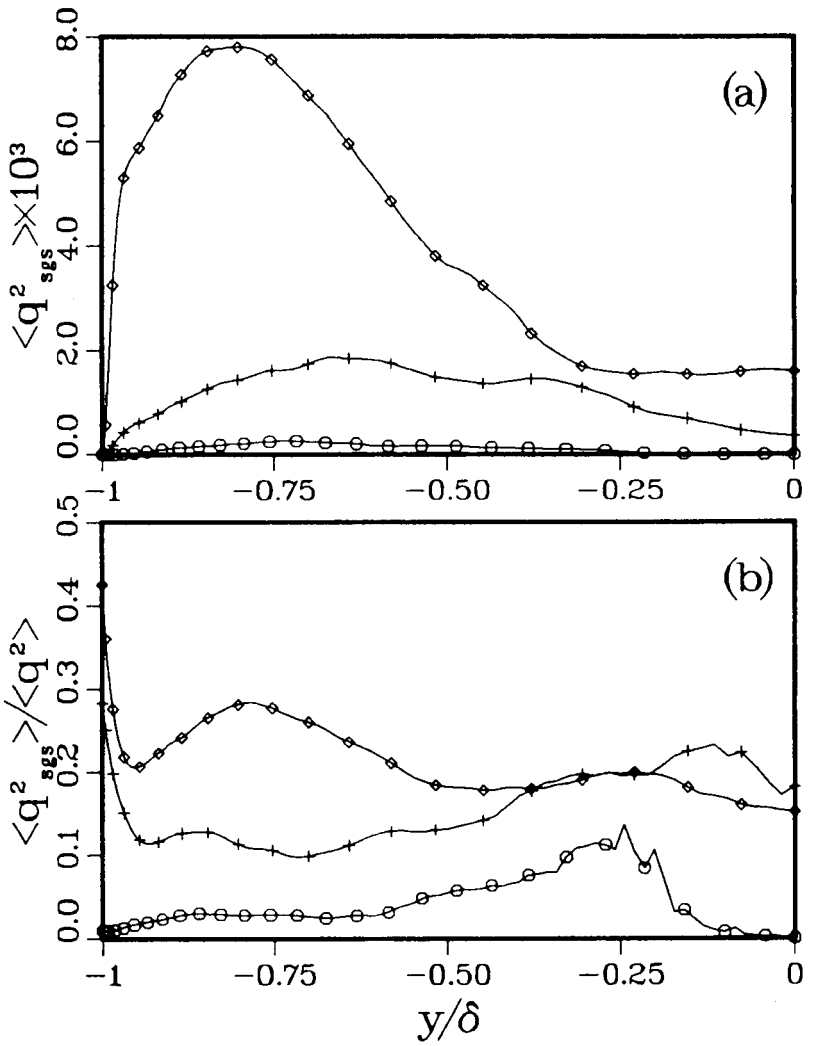

Figure 2. Subgrid scale energy and energy ratio obtained from direct simulations; $\circ$ $t = 175$; $+$ $t = 185$; $\diamond$ $t = 196$. (a) q^2_{sgs}; (b) q^2_{sgs}/q^2.

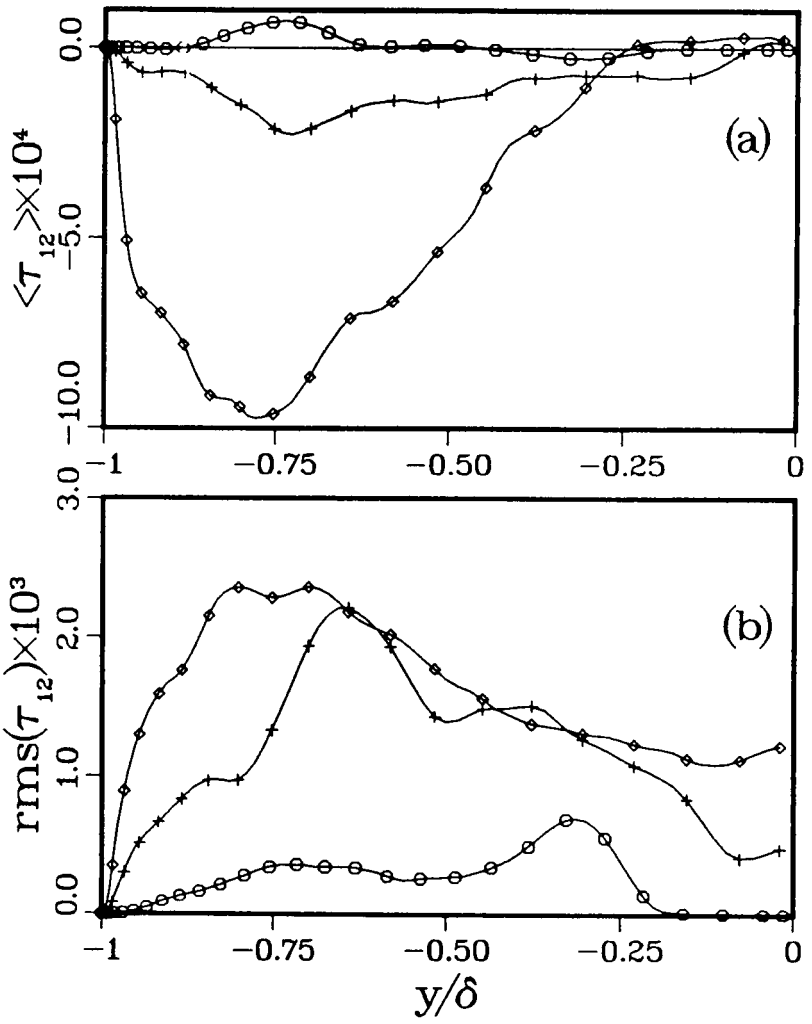

Figure 3. Residual stress τ_{12} obtained from direct simulations; $\circ$ $t = 175$; $+$ $t = 185$; $\diamond$ $t = 196$. (a) Mean; (b) root-mean-square.

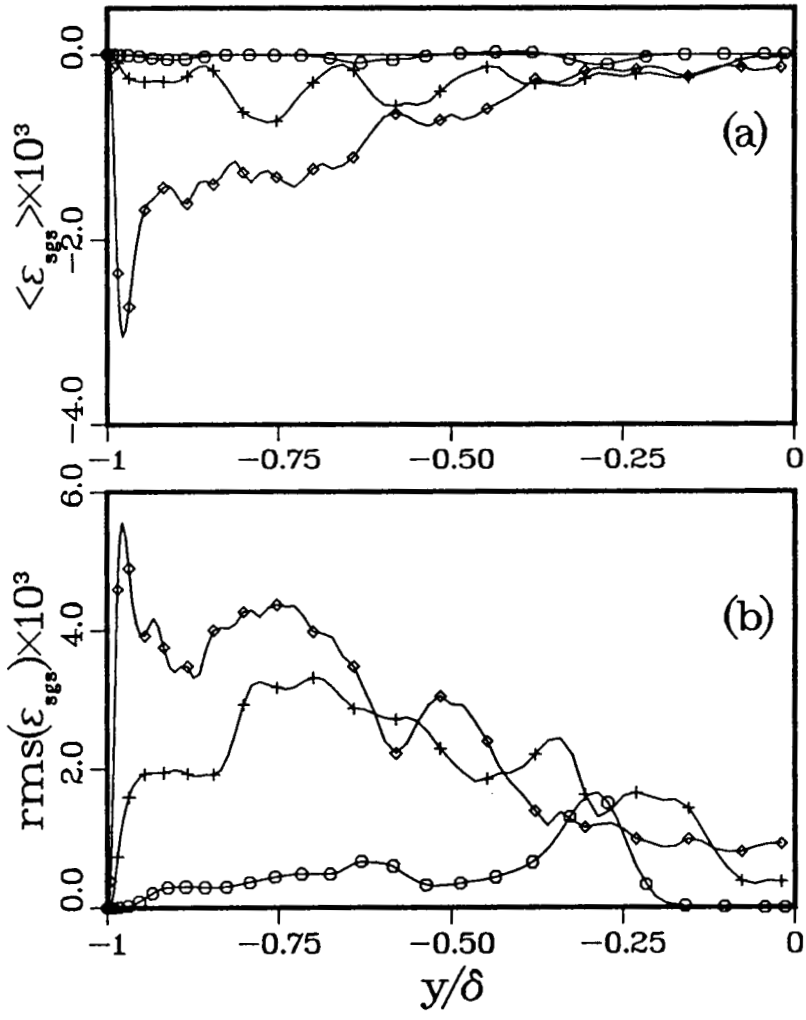

Figure 4. Subgrid scale scale dissipation ϵ_{sgs} obtained from direct simulations; $\circ$ $t = 175$; $+$ $t = 185$; $\diamond$ $t = 196$. (a) Mean; (b) root-mean-square.

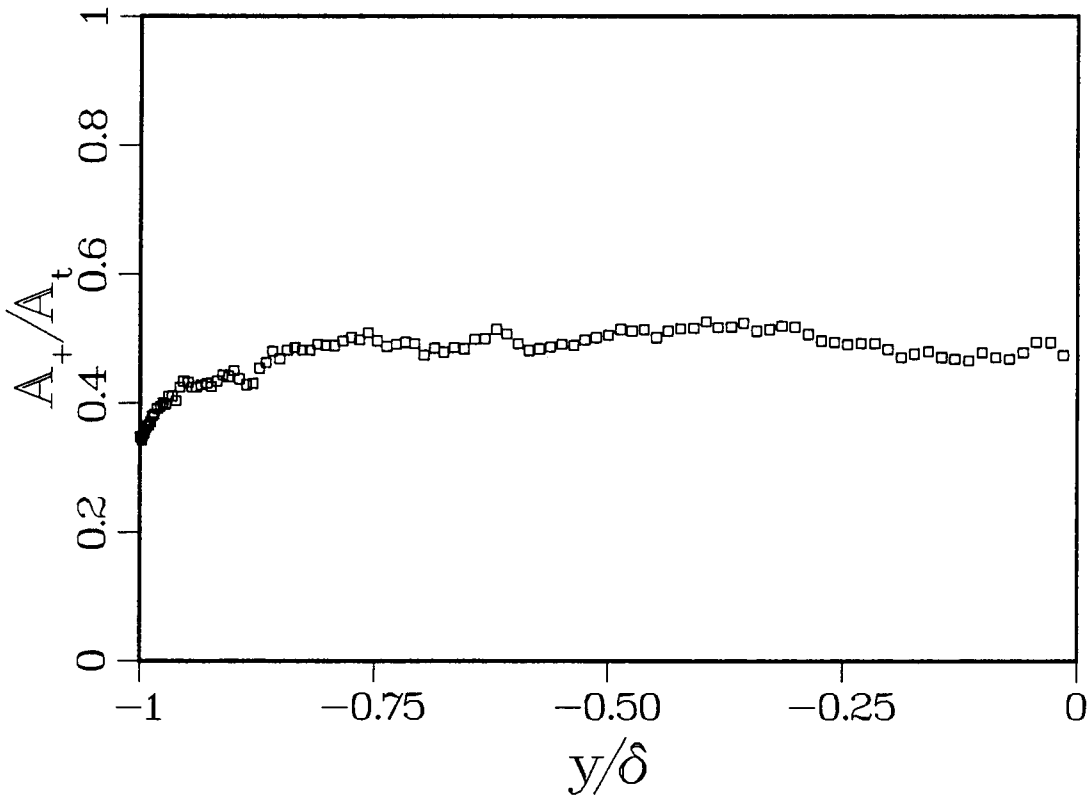

Figure 5. Ratio of the area of an xz-plane over which $\epsilon_{sgs} > 0$ to the total area of an xz-plane.

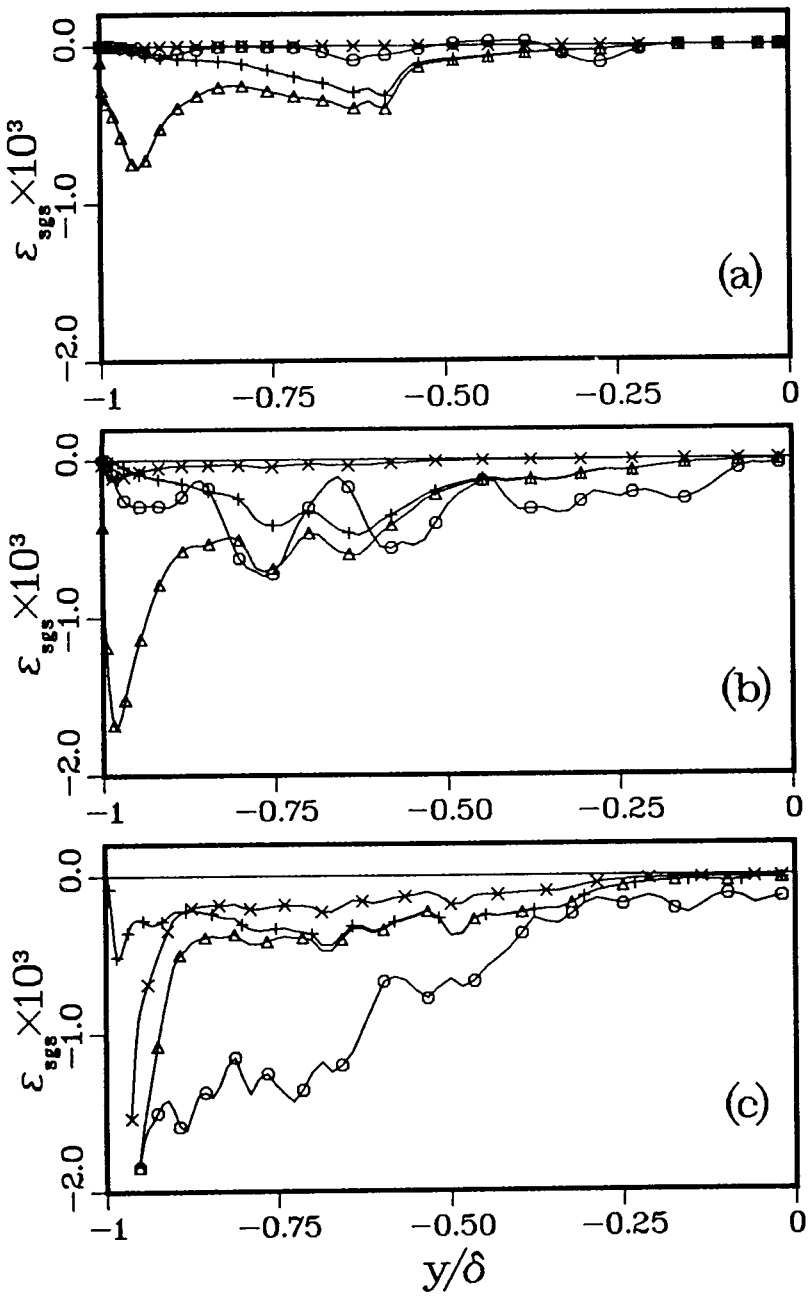

Figure 6. Subgrid scale dissipation ϵ_{sgs}; ∘ DNS; △ modeled, length scale given by (16); + modeled, length scale given by (17); × modeled, length scale given by (18). (a) $t = 175$; (b) $t = 185$; (c) $t = 196$.

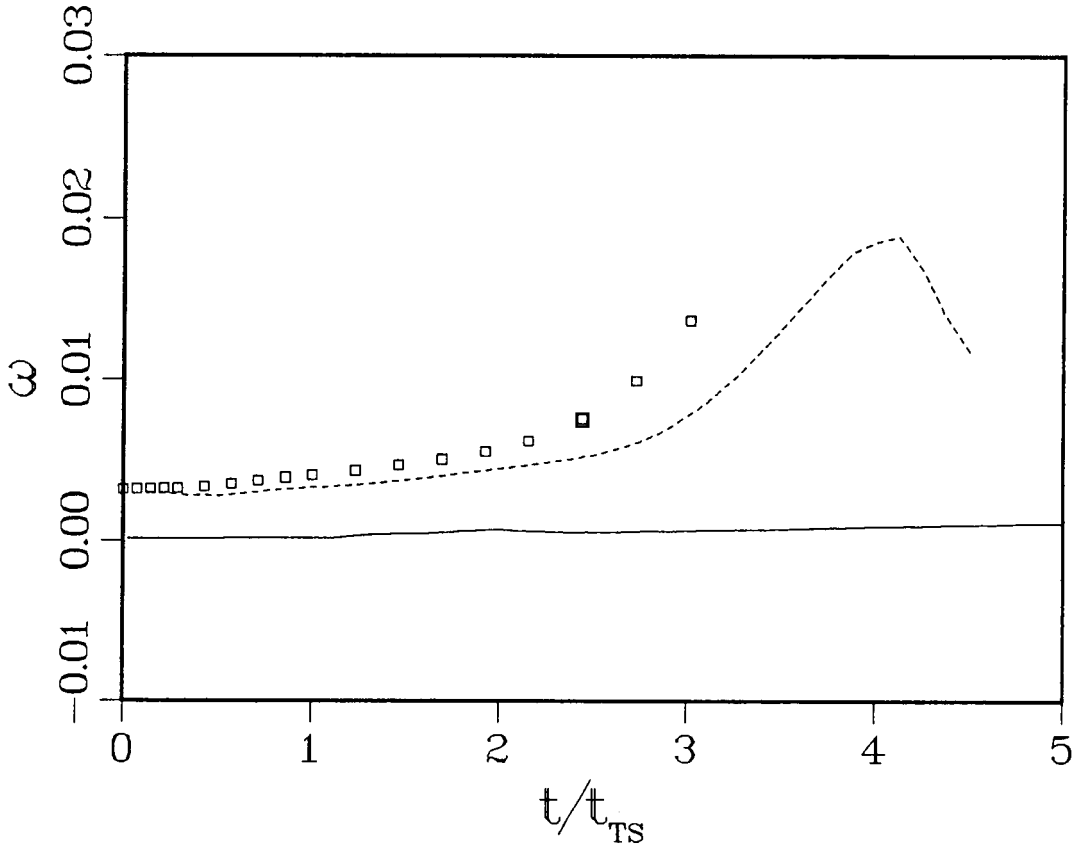

Figure 7. Time evolution of the disturbance growth rate ω. —— LES, length scale given by (18); ---- LES, length scale given by (23); ◘ DNS.

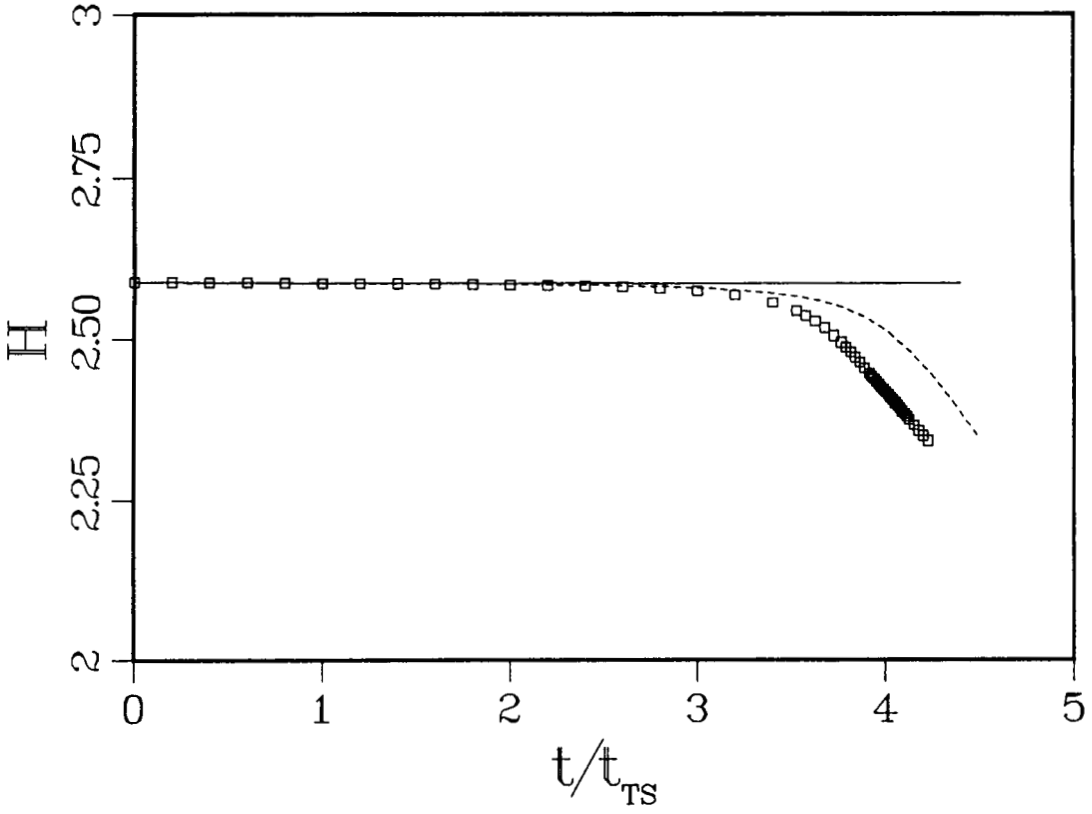

Figure 8. Time evolution of the shape factor H. —— LES, length scale given by (18); ---- LES, length scale given by (23); □ DNS.

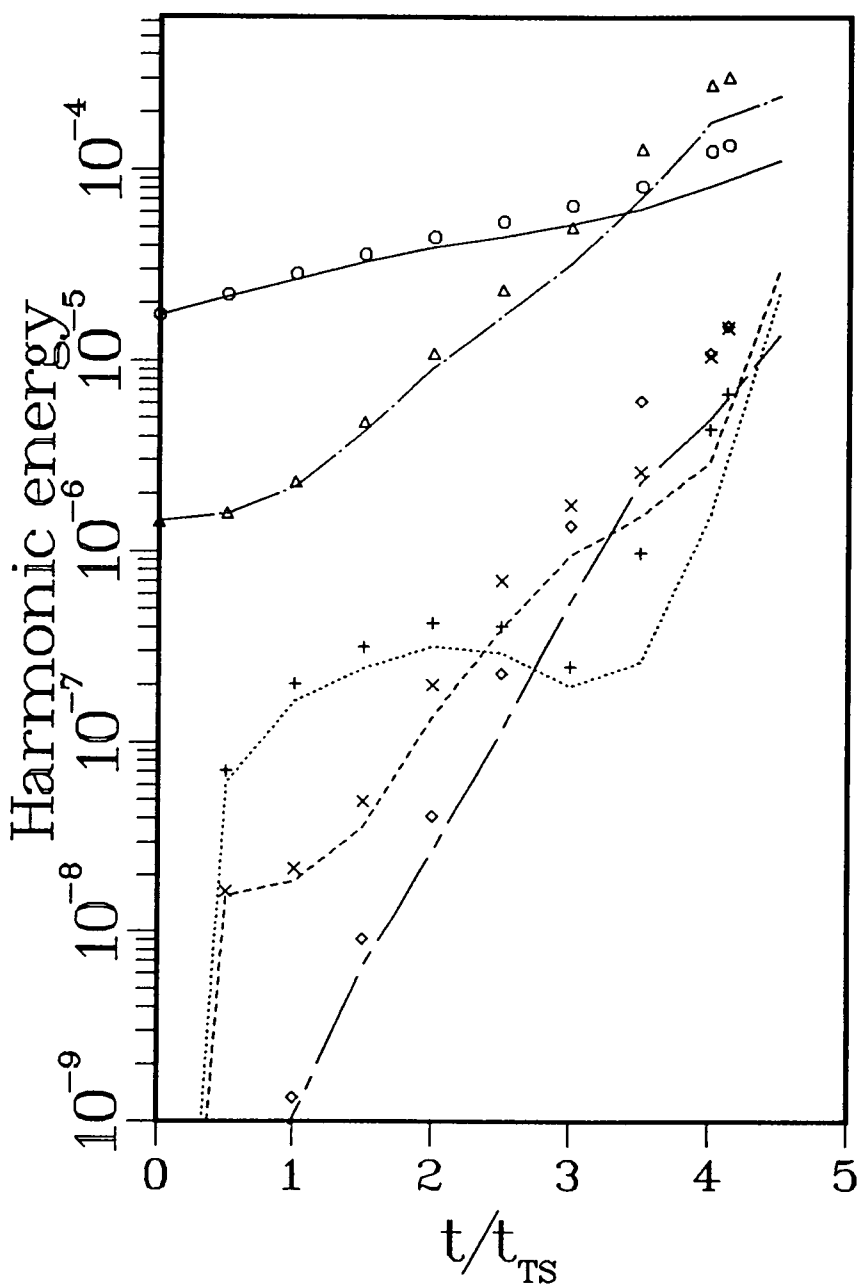

Figure 9. Time evolution of the energy content of selected harmonics. The length scale for the LES was given by (23). (1,0) mode: —— LES, ∘ DNS; (1,1) mode: —·— LES, △ DNS; (2,0) mode: ····· LES, + DNS; (2,1) mode: ---- LES, × DNS; (2,2) mode: —·— LES, ◇ DNS.

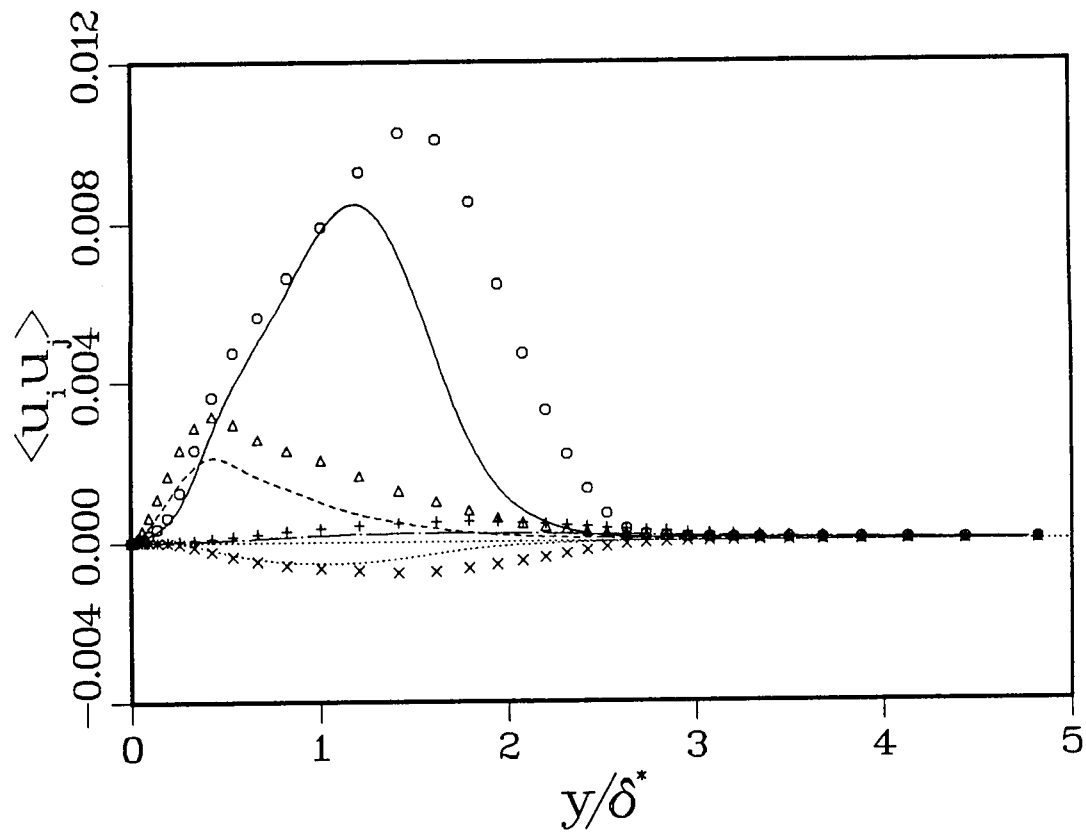

Figure 10. Large scale Reynolds stresses $< \overline{u}_i'' \overline{u}_j'' >$. The length scale for the LES was given by (23). The LES results are at $t/t_{TS} = 4$; the DNS results are at $t/t_{TS} = 3.88$ and are filtered on a 24×48×24 grid. $\overline{u}''^2$: —— LES, ∘ DNS; $\overline{v}''^2$: —·— LES, + DNS; $\overline{w}''^2$: ---- LES, △ DNS; $\overline{u}''\overline{v}''$: ····· LES, × DNS.

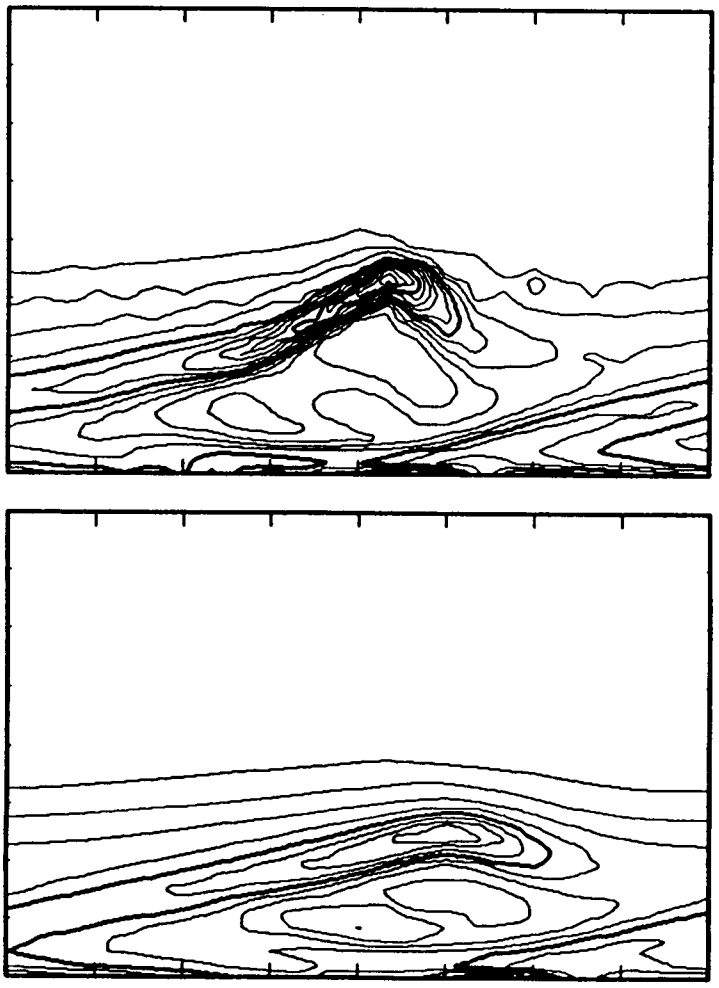

(a)

(b)

Figure 11. Contours of $\partial\overline{u}/\partial y$ in the peak xy-plane. (a) DNS at $t/t_{TS} = 3.88$ filtered on a $24\times48\times24$ grid; (b) LES at $t/t_{TS} = 4$, length scale given by (23).

NASA
National Aeronautics and Space Administration

Report Documentation Page

1. Report No.	2. Government Accession No.	3. Recipient's Catalog No.
NASA CR-181883 ICASE Report No. 89-55		

4. Title and Subtitle

ON THE LARGE-EDDY SIMULATION OF TRANSITIONAL WALL-BOUNDED FLOWS

5. Report Date

August 1989

6. Performing Organization Code

89-55

7. Author(s)

Ugo Piomelli, Thomas A. Zang, Charles G. Speziale, and M. Y. Hussaini

8. Performing Organization Report No.

10. Work Unit No.

505-90-21-01

9. Performing Organization Name and Address

Institute for Computer Applications in Science and Engineering
Mail Stop 132C, NASA Langley Research Center
Hampton, VA 23665-5225

11. Contract or Grant No.

NAS1-18605

13. Type of Report and Period Covered

Contractor Report

12. Sponsoring Agency Name and Address

National Aeronautics and Space Administration
Langley Research Center
Hampton, VA 23665-5225

14. Sponsoring Agency Code

15. Supplementary Notes

Langley Technical Monitor:
Richard W. Barnwell

Final Report

Submitted to Physics of Fluids, Series A

16. Abstract

The structure of the subgrid scale fields in plane channel flow has been studied at various stages of the transition process to turbulence. The residual stress and subgrid scale dissipation calculated using velocity fields generated by direct numerical simulations of the Navier-Stokes equations are significantly different from their counterparts in turbulent flows. The subgrid scale dissipation changes sign over extended areas of the channel, indicating energy flow from the small scales to the large scales. This reversed energy cascade becomes less pronounced at the later stages of transition. Standard residual stress models of the Smagorinsky type are excessively dissipative. Rescaling the model constant improves the prediction of the total (integrated) subgrid scale dissipation, but not that of the local one. Despite the somewhat excessive dissipation of the rescaled Smagorinsky model, the results of a large eddy simulation of transition on a flat-plate boundary layer compare quite well with those of a direct simulation, and require only a small fraction of the computational effort. The inclusion of non-dissipative models, which could lead to further improvements, is proposed.

17. Key Words (Suggested by Author(s))	18. Distribution Statement
Large-eddy simulations, transition, channel flow, boundary layers	34 - Fluid Mechanics & Heat Transfer Unclassified - Unlimited

19. Security Classif. (of this report)	20. Security Classif. (of this page)	21. No. of pages	22. Price
Unclassified	Unclassified	28	A03